

Journal of Materials Chemistry A

Accepted Manuscript



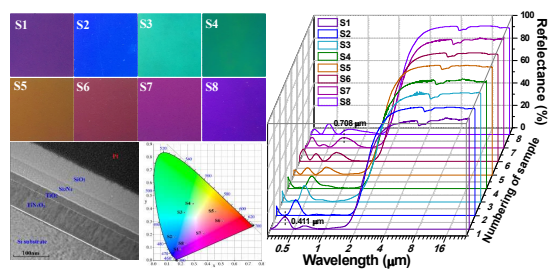
This is an *Accepted Manuscript*, which has been through the Royal Society of Chemistry peer review process and has been accepted for publication.

Accepted Manuscripts are published online shortly after acceptance, before technical editing, formatting and proof reading. Using this free service, authors can make their results available to the community, in citable form, before we publish the edited article. We will replace this *Accepted Manuscript* with the edited and formatted *Advance Article* as soon as it is available.

You can find more information about *Accepted Manuscripts* in the [Information for Authors](#).

Please note that technical editing may introduce minor changes to the text and/or graphics, which may alter content. The journal's standard [Terms & Conditions](#) and the [Ethical guidelines](#) still apply. In no event shall the Royal Society of Chemistry be held responsible for any errors or omissions in this *Accepted Manuscript* or any consequences arising from the use of any information it contains.

High-performance colored selective absorbers can simultaneously satisfy aesthetic requirements and energy performance well for architectural integration of solar applications.



Cite this: DOI: 10.1039/x0xx00000x

High-performance Colored Selective Absorbers for Architecture Integratable Solar Applications

Received 00th January 2015,
Accepted 00th February 2015Feiliang Chen^{a,b,c}, Shao-Wei Wang^{*a,b}, Xingxing Liu^{a,b,c}, Ruonan Ji^{a,b,c}, Liming Yu^{a,b}, Xiaoshuang Chen^{a,b}, Wei Lu^{a,b}

DOI: 10.1039/x0xx00000x

www.rsc.org/

Architecture integratable solar thermal technologies such as solar water heaters and solar thermoelectric generators (STEGs) rely on spectrally selective solar absorbers. These solar absorbers need to have high solar absorptivity (α) and low thermal emissivity (ε) simultaneously, which always looks dark blue or black and block the architectural integration solar applications. Colorful appearance should be taken into account for architectural integration applications. Colored absorbers with TiN_xO_y absorbing layer and $\text{TiO}_2/\text{Si}_3\text{N}_4/\text{SiO}_2$ dielectric stack are elaborately designed and can be fabricated with only two targets of Ti and Si by reactive magnetron sputtering. Both the designed and experimental results show that their color can be tuned in a huge gamut, while keeping solar absorptivity higher than 95% and thermal emissivity lower than 5%. The highest absorptivity and energy utilizing efficiency (α/ε) come to 97.6% and 27.2 respectively. They are also fabricated on thermoelectric generators to demonstrate the conversion of solar energy into electricity. The open circuit voltage dramatically increases from 171 mV to 523 mV (3.1 times) with the absorber. Additionally, the colored solar absorbers can be deposited on almost all kinds of substrates, even for flexible substrates. They can simultaneously satisfy the aesthetic requirements and excellent energy performance for architectural integration of solar thermal and thermoelectric applications, as well as other application fields.

1. Introduction

Solar energy utilizations draw huge attentions in past decades due to the serious energy crisis and environmental pollution. Solar-thermal application is one of the most important utilizing ways, including solar water heater, concentrated solar power (CSP), solar thermophotovoltaics (STPV) and solar thermoelectric generators (STEGs).¹⁻⁸ Its prospective trend is to develop solar water heater and panel solar thermoelectric generators integratable with architectures, since most of the building roofs and facades are the potential areas.^{9,10} All of these solar-thermal applications rely on solar selective absorbers,¹¹⁻¹³ which have both high solar absorptivity and low thermal emissivity, resulting in high efficiency for solar energy utilization. Although solar selective absorbers meet the architectural integration demands in energy performance, the color of most current absorbers is monotonous black or dark blue in order to obtain high solar utilizing performance. Rare color freedom blocks the architectural integration solar applications.^{14,15} 85% of architects prefer colored solar collectors other than these two colors even if losing some efficiency.¹⁶

Therefore, several approaches have been suggested to realize colored absorbers, including spectrally selective colored paints and colored solar selective absorbing coatings.¹⁶⁻²⁰ Spectrally selective colored paints can provide different colored absorbers and easy to be used. However, their absorptivity (α) is usually not high enough (less than 90% with different colors). More importantly, their thermal emissivity (ε) is very high (>30%, even larger than 40% for many colors), which results in extremely low energy utilizing efficiency (α/ε less than 3) compared with the typical values ($\alpha=95\%$, $\varepsilon=5\%$, $\alpha/\varepsilon=19$) of high performance black or dark blue absorbers. As for colored solar selective absorbing coatings, they are formed by absorbing layer itself or two absorbing layers with different component plus anti-reflection (AR) layer, or metal and dielectric multilayers. For the former, different colors will be generated by different materials and different number of layers. The absorptivity increases to 95% with increasing the number of material and layers, but emissivity increases to 9% at the same time. For the latter, the best performance of α , ε and α/ε are 94%, 5% and 18.8 generated with four layers in purple, respectively. Other colors are formed with five-layer structure and α are lower than 92%. What's more, for both of these two

schemes, the limited colors are generated from different material and different number of layers, which increases the complexity of manufacture procedure and cost.

Consequently, there are still no reported solar absorbers which can have colored appearance other than conventional black or dark blue while keep high performance of absorptivity larger than 95% and emissivity lower than 5% simultaneously. It is a challenge to make a tradeoff between the color appearance and energy performance. In this work, such aspiration can be realized based on TiN_xO_y absorbing layer and $\text{TiO}_2/\text{Si}_3\text{N}_4/\text{SiO}_2$ dielectric stack we presented. This structure is studied both theoretically and experimentally. The color appearance can be tuned in a huge wide range by changing the thicknesses of each layer, while keeping very high energy performance always. The colored solar selective absorbers are employed in panel STEGs to demonstrate their architecture integratable solar applications as well.

2. Results and discussion

2.1. Structure and model of colored solar selective absorbers

Most of the traditional solar selective absorbers reported are three-layer structure consisting of two gradient absorption layers (a high metal volume fraction layer and a low metal volume fraction layer) and a transparent AR layer.²¹⁻²³ The double interference absorption layers can maximize the absorptivity so that its reflectance spectrum is usually flat and low in visible region or only has a reflection peak in blue light and near ultraviolet region, which leads to black or dark blue color appearance. The color of the absorbers is determined primarily by the reflectance spectrum in visible wavelength range (0.38-0.78 μm). However, visible light accounts for about 50% of the sun's energy and color will cause energy loss, especially when the reflection peaks are broad and strong. That's why most of the conventional colored solar absorbers can't have colorful appearance and high performance at the same time.

To make a good balance between the energy performance and color appearance, several basic principles should be

followed to design the reflection spectrum of the colored solar selective absorber. Firstly, some reflection peaks with bandwidth narrow enough should be introduced intentionally to compose the desired color. Secondly, the energy loss and color brightness should be controlled in an acceptable range by adjusting the width and strengths of these peaks appropriately. Finally, the position of these reflection peaks should be capable of adjusting flexibly in order to produce a variety of colors. What's more, the reflection in near-ultraviolet and near-infrared should be kept as low as possible to maximize the absorption of solar radiation. A steep reflection edge should appear at near-infrared (the position of the reflection edge or cutoff wavelength relies on application temperature of the absorber) to ensure low thermal emissivity in infrared range. A reflector/absorption layer/dielectric stack structure is well consistent with the above design principle for high performance colored solar selective absorber, as shown in Fig. 1(A).

A highly infrared reflective metal substrate or metal film thicker than skin depth is on the bottom of the structure to provide low emissivity. The complex refractive index of TiN_xO_y absorption layer changes abruptly at visible wavelengths as shown in Fig. 1(B) and hence its reflectance spectrum is fluctuant. It is very useful for composing the colors and chosen as solar absorption layer. Other absorbing layers with similar property can also be used. TiO_2 , Si_3N_4 and SiO_2 are chosen as the dielectric stack layers with gradient refractive index to decrease the reflection loss of solar radiation except for the interference peaks in visible region. The optical constants of TiO_2 , Si_3N_4 and SiO_2 dielectric films in the wavelength range 0.3-2.5 μm are shown in Fig. 1(C). The refractive index of TiO_2 , Si_3N_4 and SiO_2 decreases from 3.00 to 2.30, 2.00 to 1.80 and 1.50 to 1.43 with increase of wavelength, respectively. By control the thickness of each layer, the color of such a structure can be tuned arbitrarily. Another important reason for choosing these materials is for simplicity and low cost, because all of them can be fabricated with only two targets of Ti and Si by reactive magnetron sputtering method accompanying with reactive gas of N_2 or O_2 . In this way, the setup and procedure for manufacturing these products will be largely simplified and the cost certainly lower largely as well.

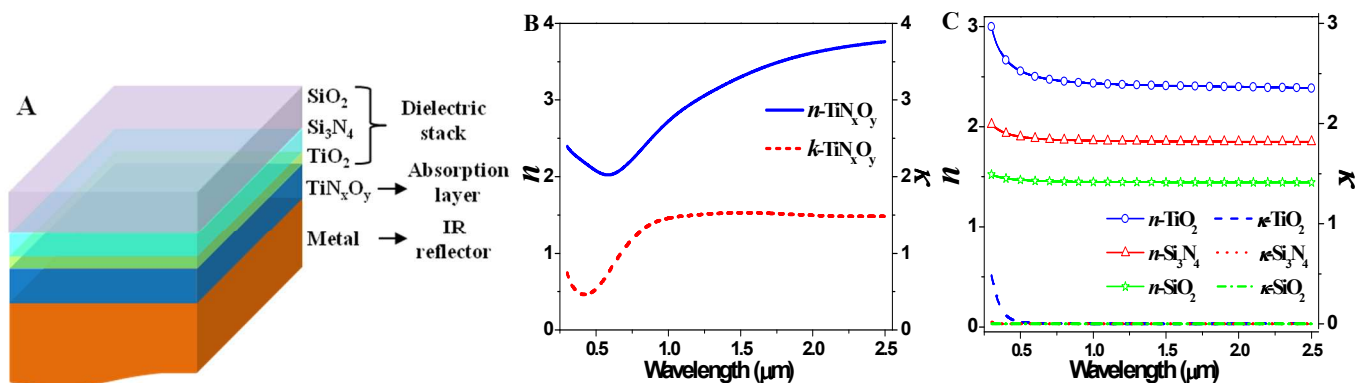


Fig. 1 (A) Schematic diagram of a colored solar selective absorber with structure of metal (IR reflector)/ TiN_xO_y /dielectric stack. (B and C) Refractive index n and extinction coefficient κ of the TiN_xO_y absorption layer, TiO_2 , Si_3N_4 and SiO_2 dielectric films.

The calculated reflection spectra of absorption layer itself and with different layers of dielectric thin films on copper substrate were compared as shown in Fig. 2 (A) to study the effect of dielectric stack. The reflectance for the absorption layer itself is on the level of 20% (corresponding to absorptivity of about 80% on opaque metal substrate), usually results in only one broad reflection peak in visible region and provides a very limited adjustable color range. When adding an antireflection dielectric thin film such as TiO_2 on it, the reflectance will be obviously lowered and the reflection peak is widened and red shift which can tune the color appearance to some extent. The reflectance will be further lowered and the reflection peak shifts red more when adding another dielectric thin film such as Si_3N_4 on the resultant structure. The color appearance can be tuned in a wider range, while reflectance loss

is still not lower enough. For the absorption layer with three-layer dielectric stack such as $\text{TiO}_2/\text{Si}_3\text{N}_4/\text{SiO}_2$, the reflectance will be much lower than the former ones and there exist at least two reflection peaks ($0.473 \mu\text{m}$ and $0.743 \mu\text{m}$) in the visible. The peaks can be easily tuned by changing the thicknesses of each layer to design for any blend colors with very high solar absorptivity and low thermal emissivity. As shown in Fig. 2 (A), the calculated solar absorptivity is greatly increased from 81% to 98% with the help of three-layer dielectric stack, accompanying with the tunability of color appearance. More layers of dielectric thin films introduced will widen the color range and promote the solar absorbing property, while increase the complicity and difficulty of fabrication. One can choose one, two, three or more dielectric layers to match different demands on color appearance and energy performance.

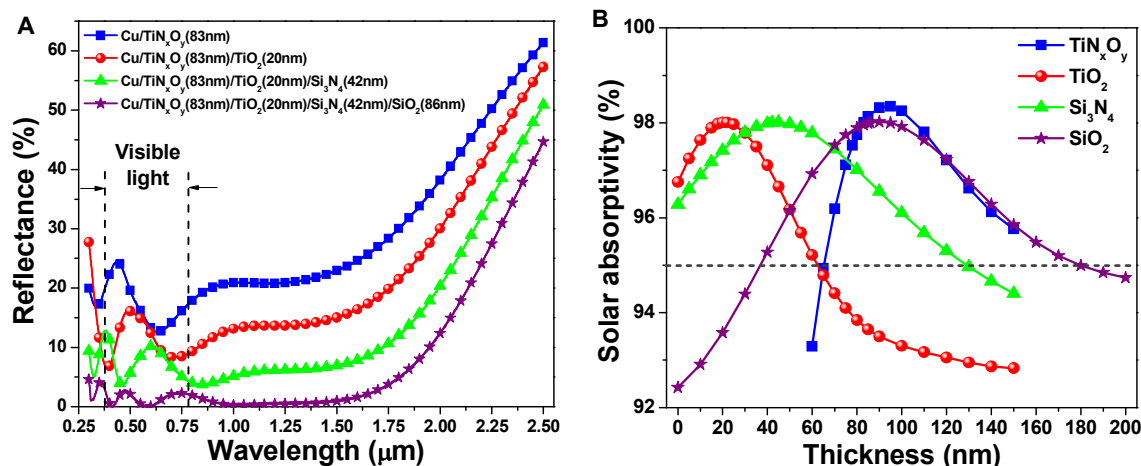


Fig. 2 (A) Comparison of calculated reflection spectra of absorption layer itself and with different layers of dielectric thin films on Cu substrate. **(B)** Dependence of the solar absorptivity on thicknesses of TiN_xO_y , TiO_2 , Si_3N_4 and SiO_2 for the optimized multilayered structure.

2.2. Theoretical design and analyses

2.2.1. Influence of each layer's thickness on absorptivity and color appearance

For the $\text{Cu}/\text{TiN}_x\text{O}_y/\text{TiO}_2/\text{Si}_3\text{N}_4/\text{SiO}_2$ solar selective absorbers, optimized multilayered structure was obtained when the thicknesses of TiN_xO_y , TiO_2 , Si_3N_4 and SiO_2 were 83 nm, 20 nm, 42 nm, and 86 nm respectively, which was used as initialization parameters for thickness adjustment. Since the emissivity is mainly controlled by the metal layer, the influence of rest layers' thickness on absorptivity and color appearance were investigated theoretically. The thicknesses of TiN_xO_y , TiO_2 , Si_3N_4 and SiO_2 were adjusted independently while other layers remain unchanged. There exists a maximum absorptivity as function of each layer's thickness and the maximum value is up to 98% as shown in Fig. 2 (B). The multilayered structure

can maintain the solar absorptivity higher than 95% in a broad range of each layers' thickness of TiN_xO_y , TiO_2 , Si_3N_4 and SiO_2 , respectively. It means that the color can be tuned by changing each layer's thickness while keeping the absorptivity on a very high level.

Correspondingly, the influence of each layer's thickness of $\text{TiN}_x\text{O}_y/\text{TiO}_2/\text{Si}_3\text{N}_4/\text{SiO}_2$ on color appearance is presented in Fig. 3 (A), (B), (C) and (D). The results show that the chromaticity coordinates of the colored absorbers can be continuously changed by tuning each layer's thickness. Most of the color coordinates are far away the neutral area (1/3, 1/3) and cover a large area of the chromaticity diagram. The combination of Fig. 2 and Fig. 3 indicates that the solar selective absorbers can be designed in a very wide color ranges with very high absorptivity by changing their thicknesses.

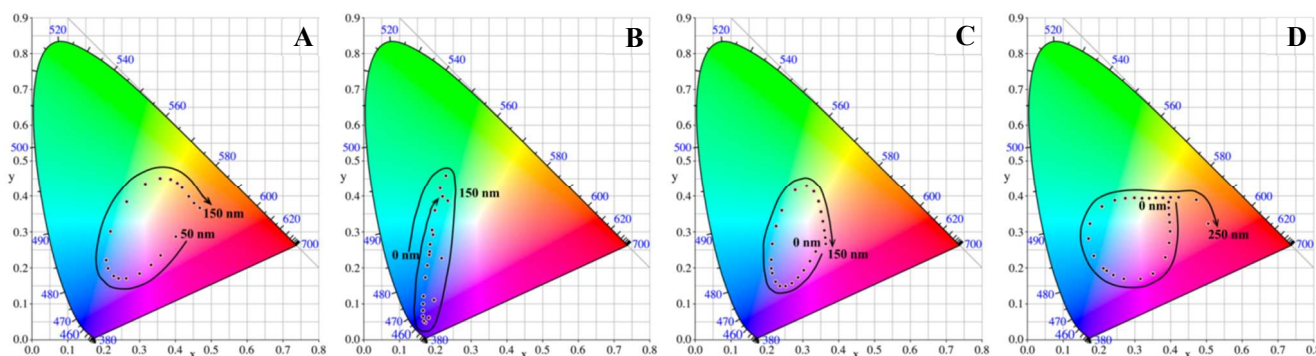


Fig. 3 Dependence of the color appearance on thickness of (A) TiN_xO_y , (B) TiO_2 , (C) Si_3N_4 and (D) SiO_2 for the multilayered structure of $\text{TiN}_x\text{O}_y/\text{TiO}_2/\text{Si}_3\text{N}_4/\text{SiO}_2$, respectively.

2.2.2. Design of colored solar selective absorbers

Considering both the color appearance and high energy performance, a series of different color solar selective absorbers were designed with different thickness combinations of the multilayered structure. Their reflection spectra are shown in Fig. 4 (A). The corresponding colors were described in chromaticity diagram as shown in Fig. 4 (B). The dominant reflection peak for color appearance can be tuned from $0.409 \mu\text{m}$ to $0.685 \mu\text{m}$, covering most of the visible region. The intensity of the reflection peaks keeps above 10% to maintain considerable color lightness. More importantly, two or more peaks

appear in the visible region and form blend colors which can expand the color to wider range. Furthermore, the solar absorptivity of all these colored selective absorbers maintain higher than 95%, since the reflectivity in near-ultraviolet and near-infrared region were suppressed as low as possible. What's more, the thermal emissivity of these solar selective absorbers is very low because the reflectivity at $2.5 \mu\text{m}$ is keeping at about 50%. The above results show that one can design almost all the color of solar selective absorbers with an absorbing layer plus three-layer dielectric stack structure, while keeping very high performance of absorptivity and emissivity.

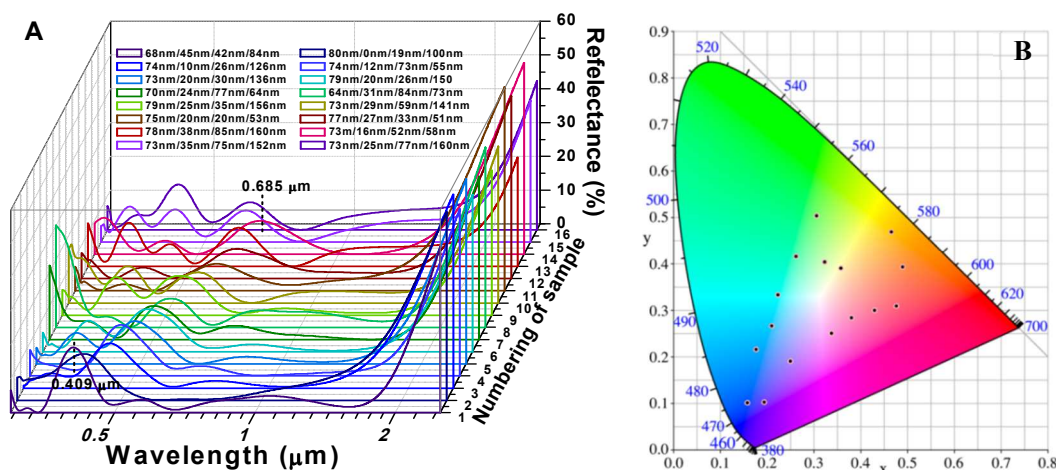


Fig. 4 (A) The calculated reflection spectra of a series of solar selective absorbers obtained by different combinations of layers' thicknesses. The horizontal axis is set as logarithmic form to highlight the visible region. (B) The corresponding color coordinates of each multilayered structure are marked on the chromaticity diagram.

2.3. Preparation of colored solar selective absorbers

Based on the above designed results, eight different colored samples were fabricated by reactive magnetron sputtering. The bright field cross-sectional transmission electron microscopy (TEM) micrograph of the multilayered structure is shown in Fig. 5 (A). Each layer and their interface can be clearly distinguished. The measured reflection spectra (from 0.3 to $25 \mu\text{m}$) of the fabricated samples on Cu substrate are presented in Fig. 5 (B). The solar absorptivity, thermal emissivity (at $100 \text{ }^\circ\text{C}$) and color lightness of these samples deduced from the measured reflection spectra are presented in Table 1. The results show that the solar absorptivity of all the samples is higher

than 95% and emissivity (at $100 \text{ }^\circ\text{C}$) lower than 5%. It is on the best level of recently reported results, such as $\text{TiAlN}/\text{TiAlON}/\text{Si}_3\text{N}_4$ tandem absorber with solar absorptance of 95% and emissivity of 7% corresponding to energy utilizing efficiency (α/ε) of 13.6,²³ and $\text{TiAlSiN}/\text{TiAlSiON}/\text{SiO}_2$ optical stack with solar absorptance of 96% and emissivity of 5% corresponding to energy utilizing efficiency of 19.2.²⁴ It indicates that the energy performance of our colored solar absorbers is competitively with conventional black or dark blue ones. The highest absorptivity and energy utilizing efficiency among these samples come to 97.6% and 27.2 respectively, even better than the reported results, especially for the energy utilizing efficiency.

Therefore, not only the color appearance range is dramatically extended with our structure, but also the performance of absorptivity and energy utilizing efficiency become even better.

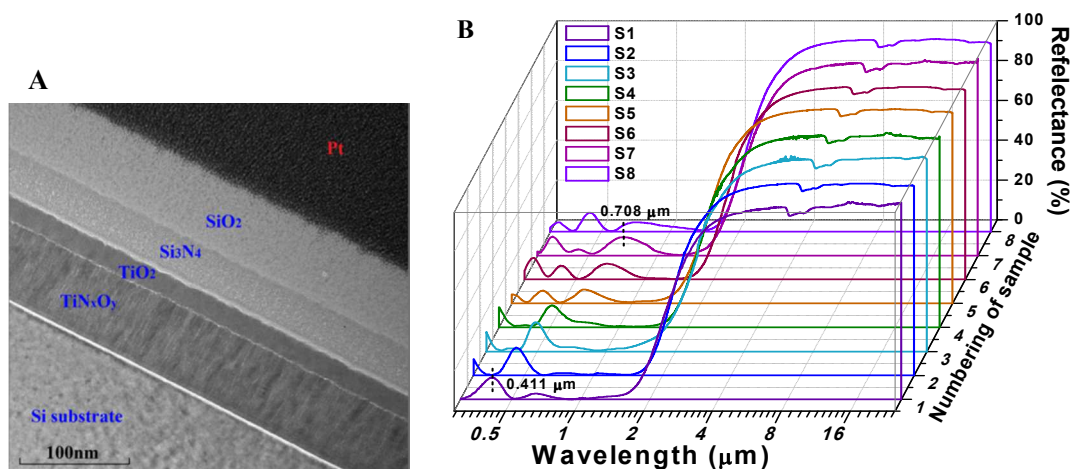


Fig. 5 (A) The bright field cross-sectional transmission electron microscopy (TEM) micrograph of the colored solar selective absorbers. **(B)** The measured reflection spectra of the fabricated solar selective absorber samples.

Table 1 Solar absorptivity, thermal emissivity and color lightness of the fabricated solar selective absorber samples.

Sample	S1	S2	S3	S4	S5	S6	S7	S8
α	97.6%	95.5%	95.3%	95.6%	95.3%	95.3%	95.0%	95.2%
ε	4.5%	4.7%	4.4%	4.6%	3.5%	4.3%	4.4%	4.5%
α/ε	21.7	20.3	21.7	20.8	27.2	22.2	21.6	21.2
L^*	11.7	21.5	32.6	32.8	22.7	17.2	19.2	13.1

Fig. 6 (A) presents the photos of the colored solar selective absorbers. The colors are violet, blue, pale green, green, yellow, red, magenta and aubergine, determining by the reflection spectra in Fig. 5 (B). There is only one main peak in visible region for the reflection spectra of sample S1, S2, S3, S4 and S7. The reflection peaks are centered at 0.411 μm , 0.460 μm , 0.491 μm , 0.511 μm and 0.710 μm , respectively, and produce the color with violet, blue, pale green, green and red. There are two main reflection peaks in visible region for S5, S6 and S8. For sample S5, the two main peaks locate at 0.410 μm and 0.610 μm and produce a blend color of yellowish-brown. For sample S6, the two main peaks located at 0.430 μm and 0.680 μm

and produce a blend of dark red. For sample S8, the two main peaks are located at 0.422 μm and 0.712 μm . The former peak is much stronger than the latter one and results in a blend color of aubergine. All the fabricated samples' color coordinates are indicated on the chromaticity diagram of Fig. 6 (B). Therefore, the absorbing layer with three-layer dielectric stack structure can form a large range of color, while keeping solar absorptivity higher than 95% and thermal emissivity (at 100 $^{\circ}\text{C}$) lower than 5%. It can match the demands of building integrated solar collectors very well and hopes to promote its application on building integrated collectors.

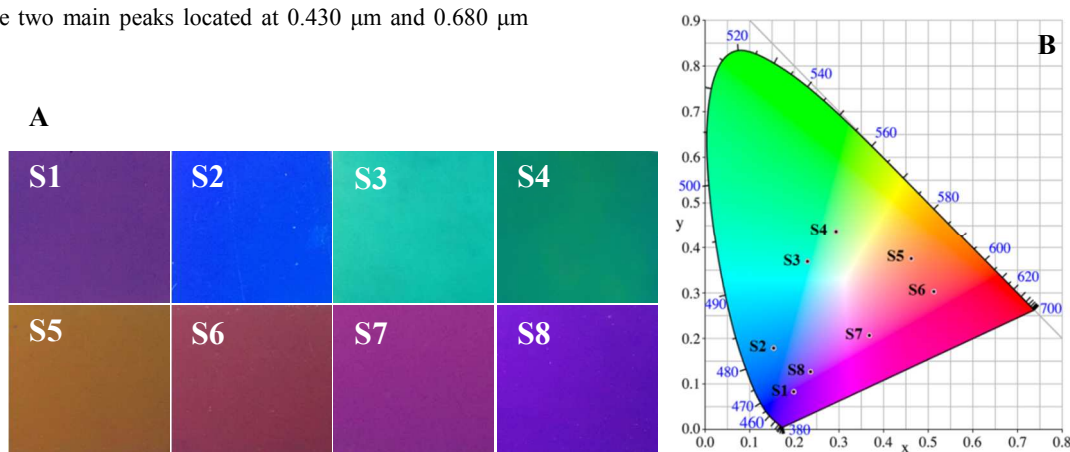


Fig. 6 (A) The photos of fabricated different colored solar selective absorbers on Cu substrates and **(B)** these samples' color coordinates indicated on the chromaticity diagram.

2.4. Panel STEGs with colored solar selective absorbers

The above results indicate that our colored solar absorbers have very high solar-thermal conversion efficiency. If they can be coated on the hot side of thermoelectric generators, then the converted thermal energy will generate electricity as well. Thus, panel STEGs are another important application field besides the solar water heater. They show a potential for co-generation of electricity and hot water.^{2,3} Their application potential will be greatly enhanced if their appearance becomes colorful to match architectures better.

To prove the application potential of colored solar absorbers on STEGs, colored solar absorbers were directly deposited on the hot side of ceramic packaged thermoelectric generators. The thermoelectric generator consists of 241 pairs of p- and n-type thermoelectric elements, with a total size of 40 mm × 40 mm. Fig. 7 (A) shows the photos of STEGs with different colored solar selective absorbers (taken in direct sunlight), including olive, hyacinthine, purple, azure, red and traditional blue. The open circuit voltages of these colored STEGs together with a thermoelectric generator without absorber (represented by 'blank' in Fig. 7 (B)) were measured by a solar simulator (Oriel Sol3A Class AAA Solar

Simulators, AM1.5, 1 kW/m²) at the same testing condition, as shown in Fig. 7 (B). The details of measuring setup and testing process were given in experimental section. The open circuit voltage of STEGs without solar selective absorbers is 171 mV. It dramatically increases to 501 mV~523 mV with the help of solar selective absorbers, which is 2.9~3.1 times of the no absorber one. The increase of about 350 mV open circuit voltage must contributed to the solar selective absorbers. They are only the initial results to prove the validity of our colored solar absorbers on STEGs. About 8% of light energy is reflected by the cover of glass on the setup. The performance should be better if the loss of light, the vacuum and thermal conductive loss are improved to enhance the temperature difference of STEGs. There is only 4% difference on the open circuit voltages of STEGs with different colored solar absorbers. It means that the energy performance of different colored solar selective absorbers is almost the same as the traditional blue absorber, which are in excellent agreement with the conclusion in section 2.3. All the above results and evidences show that the colored absorbers can help us to utilize solar energy for both thermal and electrical energies, which will be a good match for building integrated panel STEGs.

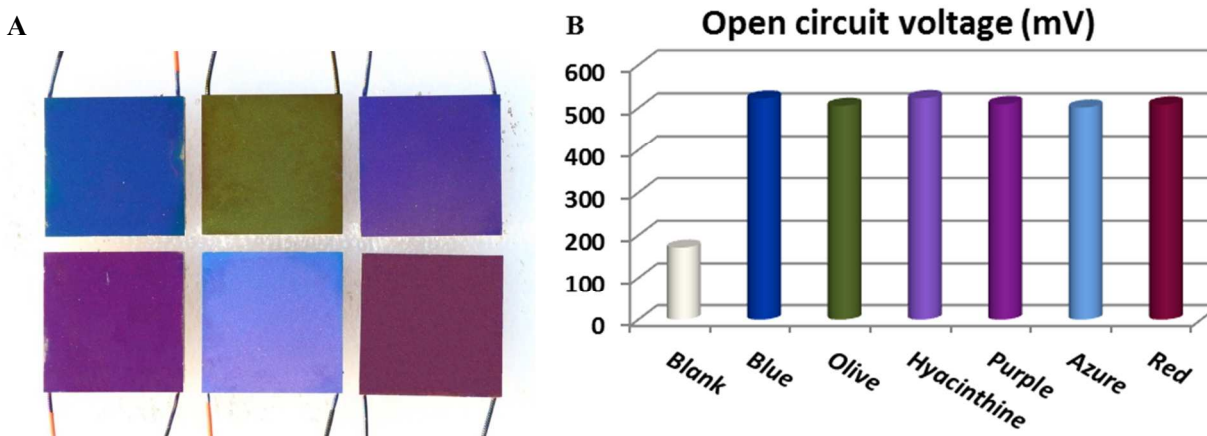


Fig. 7 (A) The photo of panel STEGs with colored solar selective absorbers (taken in direct sunlight). (B) The open circuit voltage of panel STEGs with colored absorbers, a thermoelectric generator without absorber (represented by 'blank') were measured for reference.

2.5. Colored solar selective absorbers on different substrates

The traditional substrates used for solar selective absorbers are Cu or Al which is a part of cost and confinement for their applications in different fields. However, our colored solar absorbers can be fabricated on almost all kinds of substrates with good adhesion since all the films are deposited by reactive magnetron sputtering in room temperature. In this section, we demonstrate that our colored solar selective absorbers can be deposited on different kinds of substrates including flexible substrates. The colored absorbers can be fabricated on glass with only about 150 nm thick Cu film on the bottom to obtain low emissivity in infrared. Consequently, the cost of substrates can be largely lowered by substituting metals for cheap glass. The colored absorbers can even be fabricated on different kinds of flexible substrates. The photos of colored solar selective absorbers on PET film, cotton cloth and paper substrates are shown in Fig. 8. The adhesion and uniformity are as good as on metal substrates, indicating that they can be applied in many other fields.

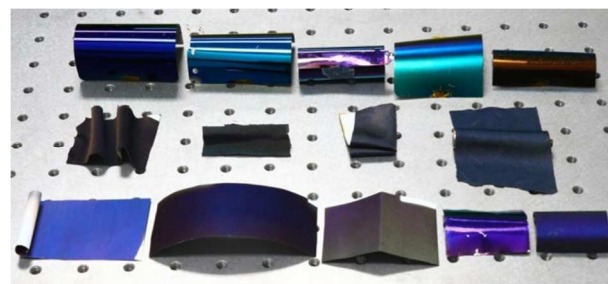


Fig. 8 The photos of colored solar selective absorbers deposited on different kinds of flexible substrates, including PET films (on the top row of the graph), cotton clothes (on the middle row of the graph) and paper (on the bottom row of the graph).

3. Conclusions

High-performance colored solar selective absorbers based on absorbing layer and dielectric stack were investigated in this article.

The $\text{TiN}_x\text{O}_y/\text{TiO}_2/\text{Si}_3\text{N}_4/\text{SiO}_2$ multilayered structure is demonstrated as an example. TiO_2 , Si_3N_4 and SiO_2 are chosen as the dielectric stack layers due to their refractive index match for anti-reflection. It is also for simplicity and low cost, because all the four films can be fabricated with only two targets of Ti and Si by reactive magnetron sputtering method. The color appearance, solar absorptivity and thermal emissivity are studied systematically with the thickness of each layer. The low reflectance of the multilayered structure and narrow reflection peaks exist in the visible are the key points for designing high performance colored solar selective absorbers. Almost all kinds of colors can be obtained while keeping high energy performance. A series of solar selective absorbers have been fabricated in colors of violet, blue, pale green, green, yellowish-brown, red and aubergine based on the above structure. Their solar absorptivity and thermal emissivity are measured to be higher than 95% and lower than 5%, respectively, which agree with the designed results very well. The colored solar selective absorbers are also fabricated on thermoelectric generators to form colored STEGs. Their open circuit voltage dramatically increases to 523 mV and is 2.9~3.1 times of the no absorber ones. Furthermore, the colored solar selective absorbers can be deposited on almost all kinds of substrates, including flexible substrates such as PET film, cotton cloth and paper. They meet the demands and are promising to promote architectural integration of solar applications such as panel solar collectors and STEGs.

4. Experimental procedures

4.1 Samples preparation

All of the films were prepared by a multi target magnetron sputtering system. Cu (99.99% in purity), Ti (99.99% in purity) and Si (99.99% in purity) targets were used in the experiments. The purity of argon, oxygen and nitrogen gases was 99.99%. The substrates were K9 glass, polished silicon wafer, polished copper, PET film, paper, cotton cloth and panel STEGs, which were cleaned with alcohol and acetone in an ultrasonic bath, rinsed with deionized water and then dried by nitrogen gas. All of the depositions were carried out under a sputtering power of 1.0 kW at room temperature and the base pressure of the vacuum chamber was 3.0×10^{-4} Pa. The thickness of the film was controlled by the sputtering time according to the deposition rate. A layer of Cu film with thickness of 150 nm was deposited first, which was prepared by DC magnetron sputtering with 30 sccm argon.

The TiN_xO_y films were prepared from Ti target with reactive gas of N_2 and O_2 . The flow rate of Ar was fixed at 30 sccm, while changing N_2 and O_2 flows to accurately control the optical property of TiN_xO_y films. The TiN_xO_y film with suitable optical constants for designing multilayered absorbers was deposited at the Ar : N_2 : O_2 flow rates of 30 sccm : 6 sccm : 3.6 sccm. The TiN_xO_y films can also be prepared from TiN target with only one reactive gas of O_2 , providing a more stable and reproducible process for controlling their property.²⁵

The TiO_2 film was deposited using Ti target by mid-frequency magnetron sputtering with Ar : O_2 flow rate of 30 sccm : 10 sccm at frequency of 30 kHz. The Si_3N_4 film was deposited using the Si target with Ar : N_2 flow rate of 30 sccm : 3.3 sccm at frequency of 30 kHz. The SiO_2 film was also deposited using the Si target with Ar : O_2 flow rate of 100 sccm : 16 sccm at frequency of 60 kHz. A film sputtered on high pressure can have low refractive index. The detailed parameters of all the deposition processes are listed in Table 2.

Film materials	Target	Sputtering power (kW)	Pulse frequency (kHz)	Base pressure (Pa)	Sputtering pressure (Pa)	Gas flow (sccm)
Cu	Cu	1.0	0 (DC)	3.0×10^{-4}	0.11	Ar=30
TiN_xO_y	Ti	1.0	30	3.0×10^{-4}	0.12	Ar: N_2 : O_2 =30:6:3.6
TiO_2	Ti	1.0	30	3.0×10^{-4}	0.13	Ar: O_2 =30:10
Si_3N_4	Si	1.0	30	3.0×10^{-4}	0.24	Ar: N_2 =50:55
SiO_2	Si	1.0	60	3.0×10^{-4}	0.27	Ar: O_2 =100:16

To ensure the experimental results agree with theoretical designed ones, the optical constants of each layer should be experimentally obtained firstly because they are different when fabricated by different methods or even by same method of different equipments. The transmission and reflection spectra of TiN_xO_y , TiO_2 , Si_3N_4 and SiO_2 single-layer film deposited respectively on K9 glass were measured. The optical constants and thickness of the single-layer films were fitted from the measured transmission and reflection spectra based on appropriate dielectric function models by film analysis and design software named 'CODE' (Coating Designer). When the fitting transmission and reflection spectra agree well with measured data simultaneously, the optical constants and thickness can be obtained simultaneously. The thickness of each single layer film were measured by stylus profiler and compared with the fitting

ones to validate the fitting effectiveness. The detailed derivation process of optical constants is presented in our other article.²⁵

4.2 Measurements and characterization

The solar energy photothermal conversion performance of solar selective absorbers is usually characterized by two basic parameters: solar absorptivity (α) and thermal emissivity (ϵ). The former was calculated in the range of 0.3-2.5 μm which covers almost all the solar radiation energy at AM1.5. The latter was calculated in the range of 2.5-25 μm at temperature of 373 K (100 °C). They are defined as the formulas mentioned in reference 25.²⁵ The appearance of colored absorbers is described quantitatively in the International Commission on Illumination (CIE) 1931 XYZ color spaces.²⁶ The gamut of all visible chromaticity on the CIE plot is a horseshoe-shaped figure shown in color. The lightness of color is described

quantitatively by L^* (ranges from 0 to 100, $L^*=0$ yields black and $L^*=100$ indicates white), which is defined in CIE 1976 ($L^* a^* b^*$), intending to mimic the nonlinear response of the eye.

Reflectance and transmittance spectra of all samples in the visible and near infrared regions (0.3-2.5 μm) were measured by Perkin Elmer Lambda 950 UV/VIS/NIR spectrometer equipped with an integration sphere. Infrared spectra of all samples were obtained with Bruker IFS 125HR Fourier transform infrared (FTIR) spectrophotometer in the range of 2.5-25 μm (4000-400 cm^{-1}). The film thickness was measured by Dektak 8 Stylus Profiler. The microstructure of the solar selective absorbers was obtained by Philips CM200/FEG Transmittance Electron Microscope (TEM).

A solar simulator (Oriel Sol3A Class AAA Solar Simulators, AM1.5, 1 kW/m^2) is used as the light source to measure the performance of colored panel STEGs. The colored panel STEGs were put in a vacuum aluminum chamber with glass cover (with average transmittance of 92%) to eliminate air convection heat leakage. The pressure of the vacuum chamber is 1×10^{-2} Pa. A circulation cooling water system was used at the bottom of the vacuum chamber for cooling the cold side of panel STEGs. The water temperature was kept at 15 $^\circ\text{C}$.

Acknowledgements

This work was partially supported by the Shanghai Science and Technology Foundations (12nm0502900, 13JC1405902), National Natural Science Foundation of China (61223006), and Youth Innovation Promotion Association CAS. The authors thank Prof. Zhifeng Li and Xin Chen, Mr. Yun Zhang and Liang Huang in our lab for the help of measuring reflectance and transmittance spectra, and Dr. Jianhua Ma for the help of measuring the performance of panel STEGs with colored solar selective absorbers.

Notes and references

^a National Laboratory for Infrared Physics, Shanghai Institute of Technical Physics, Chinese Academy of Sciences, 500 Yu Tian Road, Shanghai 200083, China.

^b Shanghai engineering research center of energy-saving coatings, 500 Yu Tian Road, Shanghai 200083, China.

^c University of Chinese Academy of Sciences, No.19A Yuquan Road, Beijing 100049, China.

E-mail: wangshw@mail.sitp.ac.cn

- 1 M. Roeb and H. Muller-Steinhagen, *Science*, 2010, **329**, 773-774.
- 2 D. Kraemer, B. Poudel, H.P. Feng, J.C. Caylor, B. Yu, X. Yan, Y. Ma, X. Wang, D. Wang, A. Muto, K. McEnaney, M. Chiesa, Z. Ren, and G. Chen, *Nat. Mater.*, 2011, **10**, 532.

- 3 J. A. Crook, L. A. Jones, P. M. Forster, and R. Crook, *Energy Environ. Sci.*, 2011, **4**, 3101-3109.
- 4 L. L. Baranowski, G. J. Snyder, and E. S. Toberer, *Energy Environ. Sci.*, 2012, **5**, 9055-9067.
- 5 M. Romeroa and A. Steinfeld, *Energy Environ. Sci.*, 2012, **5**, 9234-9245
- 6 A. Lenert, D. M. Bierman, Y. Nam, W. R. Chan, I. Celanović, M. Soljačić, and E. N. Wang, *Nat. Nanotechnol.*, 2014, **9**, 126-130.
- 7 Zhifeng Liu, Jianhua Han, Keying Guo, Xueqi Zhang, Tiantian Hong, *Chem. Commun.*, 2015, **51**, 2597-2600.
- 8 Jianhua Han, Zhifeng Liu, Keying Guo, Jing Ya, Yufeng Zhao, Xueqi Zhang, Tiantian Hong, Junqi Liu, *ACS Appl. Mater. Inter.*, 2014, **6**, 17119-17125.
- 9 A.G. Hestnes, *Sol. Energy*, 1999, **67**, 181-187.
- 10 T. Matuska and B. Sourek, *Sol. Energy*, 2006, **80**, 1443-1452.
- 11 N. Wang, L. Han, H. He, N-H. Park, and K. Koumoto, *Energy Environ. Sci.*, 2011, **4**, 3676-3679.
- 12 V. Rinnerbauer, S. Ndao, Y. X. Yeng, W. R. Chan, J. J. Senkevich, J. D. Joannopoulos, M. Soljačić, and I. Celanovic, *Energy Environ. Sci.*, 2012, **5**, 8815-8823.
- 13 F. Cao, K. McEnaney, G. Chen, and Z. Ren, *Energy Environ. Sci.*, 2014, **7**, 1615-1627.
- 14 M.C. Munari Probst, C. Roecker, *Sol. Energy*, 2007, **81**, 1104-1116.
- 15 T.N.Anderson, M.Duke, and J.K.Carson, *Sol. Energy Mater. Sol. Cells*, 2010, **94**, 350-354.
- 16 D. Zhu, S.Zhao, *Sol. Energy Mater. Sol. Cells*, 2010, **94**, 1630-1635.
- 17 Y. Wu, W. Zheng, L. Lin, Y. Qu, F. Lai, *Sol. Energy Mater. Sol. Cells*, 2013, **115**, 145-150.
- 18 Z. Crnjak Orel, M. Klanjek Gunde, M.G. Hutchins, *Sol. Energy Mater. Sol. Cells*, 2005, **85**, 41-50.
- 19 B. Orel, H. Spreizer, L. Slemenik Perse, M. Fir, A. Surca Vuk, D. Merlini, M. Vodlan, M. Kohl, *Sol. Energy Mater. Sol. Cells*, 2007, **91**, 93-107.
- 20 B. Orel, H. Spreizer, A. SurcaVuk, M. Fir, D. Merlini, M. Vodlan, M. Kohl, *Sol. Energy Mater. Sol. Cells*, 2007, **91**, 108-119.
- 21 Q. Zhang, D. R. Mills, *Appl. Phys. Lett.*, 1992, **60**, 545.

- 22 H. C. Barshilia, N. Selvakumar, K. S. Rajam, D. V. Sridhara Rao, K. Muraleedharan, A. Biswas, *Appl. Phys. Lett.*, 2006, **89**, 191909.
- 23 N. Selvakumara and H. C. Barshilia, *Sol. Energy Mater. Sol. Cells*, 2012, **98**, 1-23.
- 24 L. Rebouta, P. Capela, M. Andritschky, A. Matilainen, P. Santilli, K. Pischow, E. Ives, *Sol. Energy Mater. Sol. Cells*, 2012, **105**, 202-207.
- 25 F. Chen, S.-W. Wang, L. Yu, X. Chen, and W. Lu, *Opt. Mater. Express*, 2014, **4**, 1833-1847.
- 26 T. Smith and J. Guild, *Transactions of the Optical Society*, 1931, **33**, 73.